2020 IEEE/RSJ International Conference on Intelligent Robots and Systems (IROS)
October 25-29, 2020, Las Vegas, NV, USA (Virtual)

A Multigait Stringy Robot with Bi-stable Soft-bodied Structures in Multiple Viscous Environments

Tung D. Ta[1], Takuya Umedachi[2] and Yoshihiro Kawahara[1]

***Abstract*— The exploration of spatially limited terrestrial or aquatic environments requires miniature and lightweight robots. Soft-bodied robot research is paving ways for a new class of small-scale robots that can navigate a variety of environments with minimum influence on the environment itself. However, it is generally challenging to design miniature soft-bodied robots that efficiently adapt to the change between viscous environments. A small-scale soft-bodied robot, which could slowly move on dry land, will need rapid motions to be able to swim in a wet environment. Although using snap-through buckling of a deformable body could help to create swift motions of the robot, merely applying the snap-through buckling does not improve the swimming speed of the robot so much. Here we propose a design of a stringy soft-bodied robot that can crawl on dry surfaces and swim in liquid environments. Besides taking advantage of the snap-through buckling using coil shape memory alloys (SMAs), we design the body of the robot with a geometrical overlapping of the active body segments and control the frequency of the undulation movement, which is crucial for the swimming locomotion. We evaluate the performance of the robot in different density and viscosity liquids such as cooking oil and Glycerin solution. We found that the robot needs to drastically change its undulation from low to high frequency when it moves from high to low viscosity environments. Our robot can swim at a speed of 3.37 body-lengths per minute ($\mathrm{BL/min}$) and crawl at a speed of $1.74\,\mathrm{BL/min}$. We anticipate our findings will help shed light on the design of soft-bodied robots that adapt to the changing environments efficiently.**

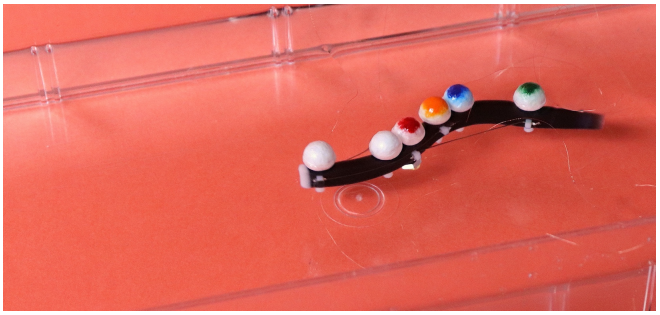

(a) Swimming in a insulator liquid (Glycerin).

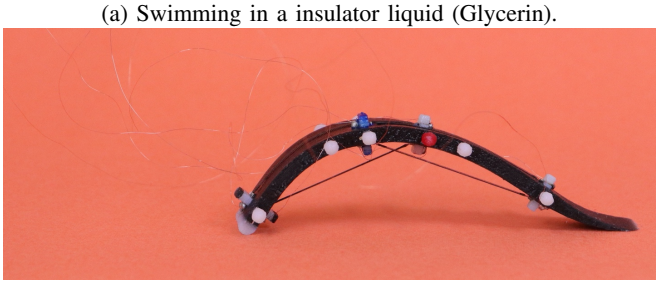

(b) Crawling locomotion gait.

Fig. 1: A multigait soft-bodied robot which swims and crawls by using the bistability of its deformable body and the geometrical overlapping of the active body segments to generate fast traveling undulation wave.

I. INTRODUCTION

Soft-bodied robots, due to their body flexibility, are poised to be great environmental adaptors. Hence, they are developed with the goal of exploring known and unknown terrestrial and liquid environments. To effectively navigate these territories, multigait locomotion with at least swimming and crawling is desirable.

In the world of rigid robots, amphibious robots are developed using multiple limbs as legs or fins [1], [2], [3]. Other robots have flexible membranes that act as long fins that support both locomotions underwater and on dry land [4], [5]. However, these robots are bulky, which makes it challenging to get into narrow spaces. Another approach is to make slender amphibious robots that are inspired by the locomotion of salamander [6] or snake [7], [8]. These robots consist of multiple rigid links to mimic the undulation of the reptiles. However, the rigidness of the links reduces its adaptability and makes it challenging to miniaturize.

Even though there is a lot of research on the fabrication and controlling of deformable sensors and actuators in soft robotics, the application of soft-bodied robots in amphibious environments is not well investigated. Robots as in [9], [10] are soft-bodied amphibious robots because they can crawl on dry land and the floor of the liquid bath. However, these robots do not know how to swim, so their applications are limited. Therefore, swimming capability is crucial for building high performance amphibious soft-bodied robots.

A. Swimming

For the better design of robotic underwater locomotion, a lot of researches is focusing on studying the aquatic locomotion and its kinematic/dynamic. For *carangiform* swimming (fish-like swimming), the research in [11] shed light on the hydrodynamic of a mackerel-like flexible body using numerical investigation simulation. As for *anguilliform* swimming (eel-like undulation swimming), the research in [12], [13] analyzed the wake structures and hydrodynamic of a swimming eel/lamprey-based robot. The research showed that different

*This work was supported by JST ERATO Grant Number JPMJER1501, Japan.

[1]Graduate School of Engineering, The University of Tokyo, 7-3-1 Hongo, Bunkyo-ku, Tokyo, Japan {tung, kawahara}@akg.t.u-tokyo.ac.jp

[2]Falcuty of Textile Science and Technology, Shinshu University, 3-15-1 Tokida, Ueda, Nagano, Japan umedachi@shinshu-u.ac.jp

models of the passive tail result in different wake structures, which affects the swimming speed of the eel/lamprey-based robot. Hirata in [14] gave a summary of the principle of the fish locomotion in robotic applications.

Swimming robots, especially the soft-bodied robots, are taking inspiration from the structure of aquatic creatures such as fish, eel, and lamprey. The robots in [15], [16] can effectively swim underwater by mimic the locomotion of a fish escaping a predator or the swimming gait of a manta-ray. The *anguilliform* locomotion of eels or lampreys inspired the robots in [17], [18].

One of the keys to making swimming soft-bodied robots is to choose a suitable actuator. The soft robotic fish in [19] and [20] used a combination of a pneumatic/hydraulic actuator to actuate the robot fish in escape wake. This actuator is only efficient for medium-sized swimming robots as it has to house a compressor to supply pressure to the actuator. Other swimming robots, such as ones in [21] and [16] used dielectric elastomer actuators to generate the flapping motions of the caudal and wing fins of the robot fish to propels it forward. A disadvantage of the dielectric elastomer actuator is that it requires a complicated controlling circuit board under high voltage input ($10\,\mathrm{kV}$) to generate meaningful locomotion gaits. The development of shape memory alloys (SMA) makes it easily accessible to many researchers. Thanks to its compactness, SMAs are used widely in making swimming robots such as starfish-liked robot [22], SMA actuated fish robot [23], [24], and turtle soft robot [25].

B. Terrestrial locomotion

The terrestrial locomotion of soft-bodied robots is more thoroughly studied than swimming soft-bodied robots. By using pneumatic actuators, a soft-bodied robot can move with multiple locomotion gaits [26]. Other soft-bodied robots can navigate the environment by growing [27]. The robots in [28] use shape memory alloys (SMA) to actuate and generate different locomotion gaits inspired by the locomotion of caterpillars. Using SMAs in a soft-bodied robot is convenient as it does not add too much overload to the robot, and the controlling mechanism is also simple (as shown in [29], [30]).

However, although the SMA can contract quickly, it is generally taking a long time to cool off and return to the resting length. This disadvantage makes it challenging to apply SMA in small scale swimming robots, which require fast motion to propel its body forward. Nishikawa *et al.* in [31] proposed using snap-through buckling with SMAs to make jumping robots. However, the movement of the snap-through buckling in this jumping robot is hard to control and generally happens spontaneously. Besides, not only the behavior of the snap-through buckling in higher viscosity environments is not elucidated, our preliminary experiment suggests that merely using the bistable structure is not enough to generate efficient swimming gait.

In this paper, taking advantage of the snap-through buckling with SMAs, we propose the overlapping bistable structure to make a small scale soft-bodied robot that can crawl and swim. Our contributions include:

- Design of swimming and crawling soft-bodied robot based on overlapping snap-through buckling to generate fast traveling undulation mechanical wave along a bistable deformable beam,
- Evaluation of the locomotion gait, crawling, and swimming speed of the small scale stringy soft-bodied robot in different viscosity.

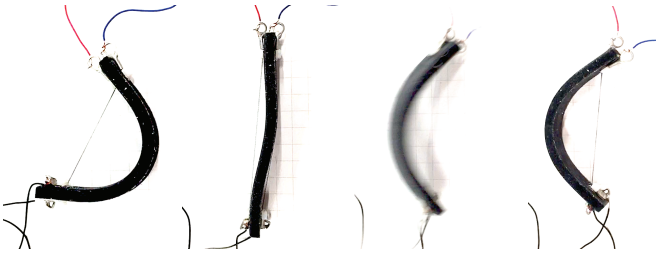

Fig. 2: Serial photo-shoots of a snap-through buckling of a $50\,\mathrm{mm} \times 10\,\mathrm{mm} \times 3\,\mathrm{mm}$ elastic beam. The snap-through happens in a fraction of a second (about $10\,\mathrm{ms}$).

II. SOFT-BODIED ROBOT DESIGN

In this paper all of the mechanical components of the robot are printed using the multi-material inkjet 3D printer Objet 260 Connex3™. Rigid parts are printed with polypropylene plastic-like material VeroWhite™. Soft and elastic parts are printed with rubber-like material TangoBlackPlus™. All the mechanical properties of these materials can be found on the website of the provider[1].

A. Snap-through Buckling of An Elastic Beam

The snap-through buckling [31] of a flexible beam happens when there are different magnitude axial bending compression at both sides of the beam. Depending on the characteristic of the beam, such as dimensional and mechanical properties, the snap-through buckling will happen differently. In our setup, we use two SMAs S_0 and S_1, which are oppositely attached to the two sides of the beam to generate the axial bending compression at both sides of the beam (as shown in Fig. 2). The activating time-span of each SMA is t_s. We can induce the snap-through buckling of the beam by activating the two SMA with an overlapping time $t_b \leq t_s$. When t_b is negative, it means there is no overlap between the two SMAs, and the time gap between the ending and the starting of the two SMA is $|t_b|$. Fig. 2 shows the real snap-through buckling of an elastic beam. The buckling duration is about $10\,\mathrm{ms}$. We will use this elastic beam as the building block to design our multigait soft-bodied robot.

B. 2-segment Soft-bodied Robot

We are aiming at building a small scale soft robot that can navigate spatially limited spaces. To fulfill this goal, one of the most simple body structure is the eel-like stringy beam. This structure allows the robot to move on land and swims in liquid environments, just like eels, lampreys,

[1] https://www.stratasys.com

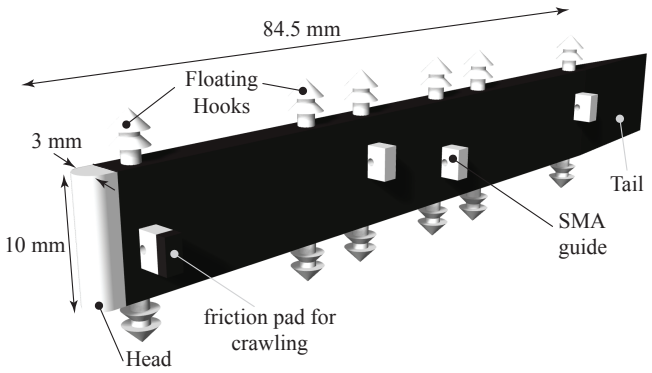

Fig. 3: Our robot is a stringy robot which comprises an $84.5\,\mathrm{mm} \times 10\,\mathrm{mm} \times 3\,\mathrm{mm}$ slender elastic beam as main body, rigid guides to attach four SMAs, 12 rigid hooks to attach buoyancy elements. The body of the robot is designed to streamline the liquid flow during swimming. The head and the first SMA guide is specially designed to implement the switch of static friction coefficient which supports terrestrial crawling.

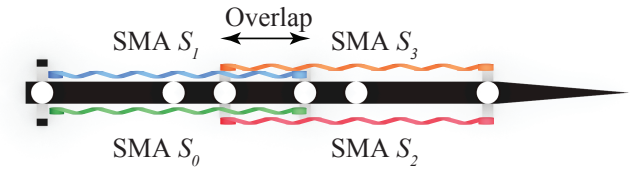

Fig. 4: Four SMAs are attached to the 2-segment body. By deliberately actuating these SMAs, we can bend the body segments to generate traveling mechanical wave along the body beam.

TABLE I: Robot design specification

Parameter	Value
Robot dimension $l \times h \times w$	$84.5\,\mathrm{mm} \times 10\,\mathrm{mm} \times 3\,\mathrm{mm}$
Active length	$l_a = 62\,\mathrm{mm}$
Coil SMA	BioMetal Helix BMX100
SMA coil diameter	$d_s = 0.4\,\mathrm{mm}$
SMA standard drive current	$150\,\mathrm{mA}$
SMA phase change temperature	$\approx 50\,^{\circ}\mathrm{C}$
SMA resting length	$l_s = 0.6l_a = 37.2\,\mathrm{mm}$

snakes, or caterpillars. For the creatures with a long body and non-developed limbs, locomotion modes can be undulating, rectilinear, or inching. Especially, the undulation is also beneficial to aquatic creatures, like eels, to navigate the underwater. Therefore, we will design our robot for crawling on land as a caterpillar but swim like an eel (*anguilliform* locomotion). Fig. 3 shows the 3D model of the robot, and Fig. 1 shows the really printed robot.

1) Swimming Design: In a liquid environment, the propulsive thrust is generated by the reaction forces of the surrounding liquid to the undulating body. As pointed out, in [32], with soft-bodied robots, a 2-link or 2-segment body structure is enough to generate a pseudo-sinusoidal traveling wave, which supports the locomotion. Therefore, we design the robot to have a 2-segment body which is actuated by four SMAs. However, in our preliminary experiments, even with fast motion using bistability, a two-consecutive-body-segment robot is poor at swimming. The robot needs a smooth retrograde wave to improve the swimming speed. Inspired by the overlapping muscular arrangement in fishes [33], we achieve this retrograde wave by putting the two-segment with a geometrical offset (overlapping) of the SMAs, as shown in Fig. 4. Let l_a be the length of the robot, which can be actively bent. The overlapping length is $l_{offset} = 0.2l_a$.

As mentioned in [13] and [14], because the passive tail is essential to generate the propulsive thrust, we designed the body beam to be tapper-ed in the end. This tapper part will act as a passive tail for our robot. For making the robot float in a liquid environment, we design hooks along the body to attach necessary buoyancy elements. The buoyancy elements are Styrofoam spheres with a diameter of $8\,\mathrm{mm}$. Depending on the density of the liquid, we can add or remove the buoyancy elements.

2) Crawling Design: In a terrestrial environment, we make the head of the robot from a low friction material (VeroWhite™), and the first SMA guide is covered by a high friction material (TangoBlackPlus™). This configuration enables the switching between high and low friction during the crawling cycle of the robot [28].

3) Actuation: Our robot will swim and crawl by bending its body segments. We use four coil SMAs (BioMetal Helix BMX100[2]) which are attached to both sides of the 2-segment body (as shown in Fig. 4). The length of each SMA depends on the length of a body segment and is set to be $l_s = 0.6l_a$ in the configuration of our robot. Table I lists the design specification of the robot. The parametric design of the robot could be found in our repository[3].

C. Locomotion Gait Generation

Our robot uses the same body structure and actuator configuration for navigating both terrestrial and liquid environments. By controlling the actuators differently, we generate different modes of swimming and crawling.

1) Swimming: One of the most efficient ways for a long beam to swim in a liquid environment is to undulate its body parts continuously to generate a propulsive thrust. For a 2-segment body to undulate with four SMAs, we timely activate the SMAs to bend the body segments serially. Fig. 5 shows the time control of the SMAs contraction and expansion. Table II lists out the parameters for controlling the undulation. The bending curvature of a body segment depends on the activating time t_s of the SMA and the pulse width modulation PWM, which is used to control the electric current fed to the SMA. The overlapping-time t_{oi} of the SMA S_i will control the speed of the traveling wave. To control

[2]https://toki.co.jp/biometal
[3]https://github.com/KawaharaLab/soft-amphibian

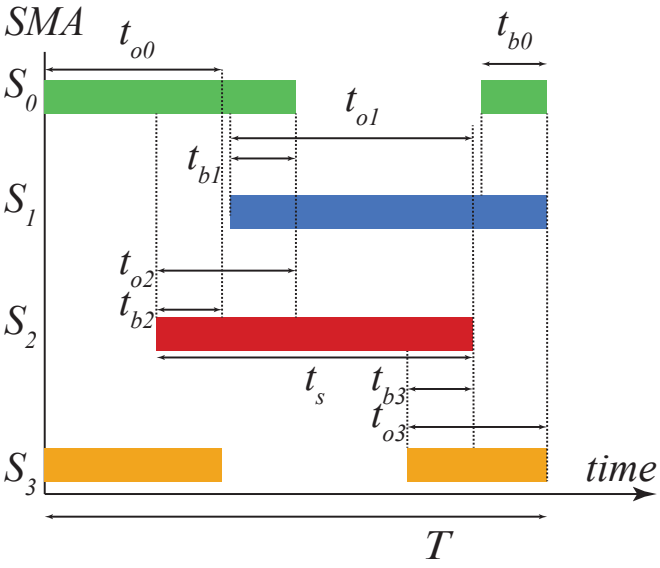

Fig. 5: Controlling pattern for actuating four SMAs to generate swimming undulation.

TABLE II: Setup value of controlling parameters

Parameter	Value
SMA on-time t_s	200 ms - 1000 ms
SMA S_i overlapping-time	$t_{oi} = 0.5t_s$
SMA S_i bistability-time	$t_{bi} = \{-1.0, \pm 0.3, \pm 0.2, \pm 0.1, 0.0\}t_s$
PWM for SMA	255

the snap-through buckling, we use the bistability-time t_{bi}, which is the overlapping time between the SMA S_i and its opposite SMA.

In this setup, we make the robot float in the liquid environment using $8\,\mathrm{mm}$-spherical buoyancy elements made of Styrofoam. The number of buoyancy elements can be adjusted depending on the density of the liquid.

2) Crawling: With the same undulation manner, a slender beam can crawl on the terrestrial surfaces. However, as studied in [32] and [34], the anisotropic frictional surface is needed for the robot to undulate forward. It is challenging to design such a surface with the miniaturization of our robot. A simpler and better way for a robot this small size to crawl is to mimic the inching gait of a caterpillar [28]. Fig. 6 shows the model of crawling with the frictional mode alternation at the head and the tail of the robot. As mentioned in II-B, we print the head of the robot with low friction material and the first SMA guide cover with high friction material. During the bending of the first body segment, the ground touching point will be alternated between the head and the first SMA guide. Another frictional alternation necessary for the crawling of the robot is the switching between the tail and the last SMA guide. Here, we print the tail with high friction material and the last SMA guide with low friction material. The coordinately frictional switching at the head and the tail will push the robot to crawl forward.

In the crawling mode, we remove the buoyancy elements

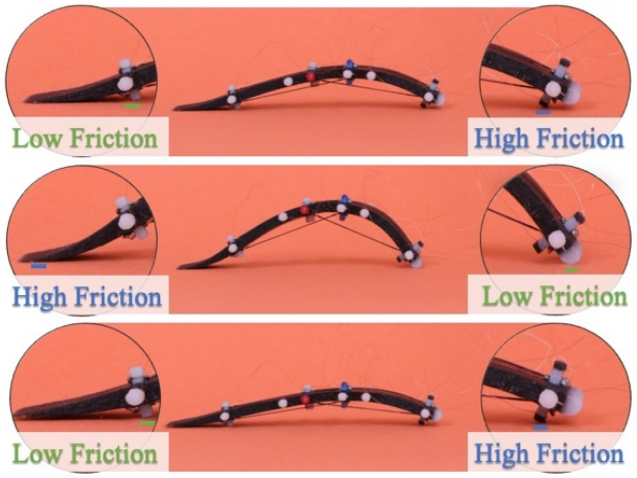

Fig. 6: Our robot crawls by inching its body and alternating the frictional mode of the head and the tail to move forward.

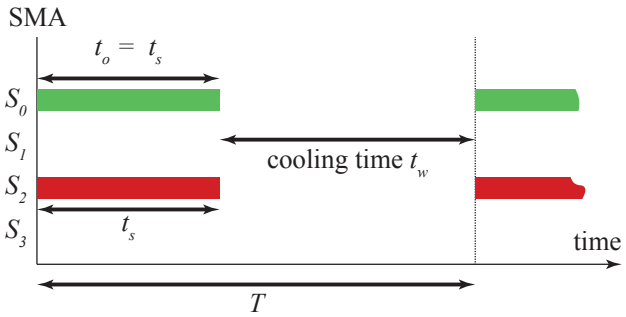

Fig. 7: We timely control the SMAs to generate inching locomotion gait. Only the SMA pair facing the crawling surface will be controlled; the other SMAs are left undriven.

and orient the robot to be a flat elastic beam parallel to the ground (in swimming mode, the robot is perpendicular to the liquid surface). The SMA actuators are controlled sequentially, as shown in Fig. 7. The crawling locomotion has the same controlling parameters as that of the swimming. Table II lists out these parameters. The difference between the two modes is that in the inching fashion, we only drive the SMA pair, which is facing the ground (S_0 and S_2 in Fig. 6). The SMA pair which is not facing the ground (S_1 and S_3) will be left un-driven. The robot uses the elastic energy of the beam and its own weigh to extend the contracted SMAs. It is possible to accelerate the extension of a contracted SMA by contracting the opposite SMA. However, as it requires fine-tuning the controlling parameters, this acceleration will be left for future works.

III. EXPERIMENT

In this section, we will evaluate the performance of our robot in terms of locomotion speed. We control the robot in an open-loop fashion using an Arduino board. The robot and the controlling board are driven by a $18\,\mathrm{V}$ DC power supply (AD-8722D). To minimize the mechanical influence of the tethering wires, we connect the robot to the controlling board

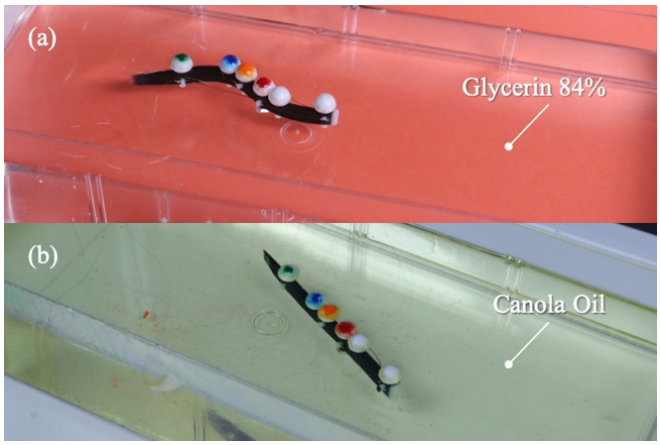

Fig. 8: The robot swims in insulator liquid baths to prevent shorted circuit. (a) Swimming in Glycerin 84%, (b) Swimming in Canola Oil.

TABLE III: Swimming environments at 25 °C

Name	Density	Absolute Viscosity
Canola Oil	0.90 g/cm^3	46.20 mPa · s
Glycerin 84%	1.21 g/cm^3	110.04 mPa · s

using 40 cm long polyurethane enameled ϕ0.05 mm copper wires and the controlling board is put 30 cm above the robot. The experiment is filmed using a web camera (Logitech HD Pro Webcam C920[4]). The locomotion of the robot is evaluated using our in-house OpenCV object tracker.

A. Swimming

1) Experiment Setup: We test the swimming performance of our robot in a liquid bath at room temperature (25 °C). At this stage, because our robot is not electrical insulated, to prevent shorted circuits, we can only use liquids that are insulators. To evaluate the influence of the liquid viscosity on the swimming performance, we let the robot swim in vegetable oil (Canola Oil) and Glycerin solution (Glycerin 84%), as shown in Fig. 8. Table III shows the properties of these two liquid at room temperature (25 °C).

We evaluate the undulation swimming of the robot based on changing the parameters in Table II. According to our preliminary test, with the input voltage of 18 V, a 37.2 mm long BMX100 SMA which is submerged in cooking oil or Glycerin can be driven stably for 1000 ms. However, repeatedly heating up the SMA for long period of time will make the SMA wear-out quickly. Therefore, we set the limit to $100\,\text{ms} \leq t_s \leq 1000\,\text{ms}$. The overlapping time are set equally to all SMAs, $t_{oi} = t_o = 0.5t_s$. With an assumption that four SMAs are created equally, we set bistability-time $t_{bi} = t_b$ with possible values as shown in Table II. Based on the time controlling mechanism as shown in Fig. 5, the period of the undulation is $T = 2t_s(1 - t_b)$.

[4]https://www.logitech.com

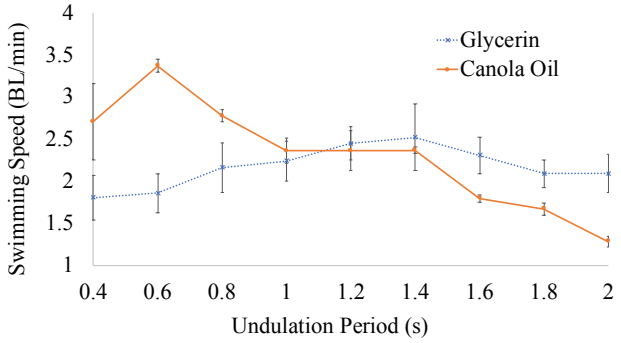

Fig. 9: The swimming speed (BL/min) of our robot varies depending on the period of the undulation.

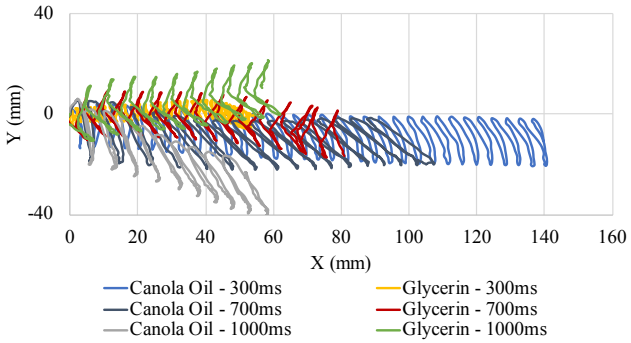

Fig. 10: The swimming trajectories of our robot in Canola Oil and Glycerin bath. Trajectory of the robot swimming in Canola Oil with SMA activation time $t_s = 300\,\text{ms}$ is stable and straight. The robot with $t_s = 700\,\text{ms}$ which swimming in Glycerin solution also has a stable trajectory. In contrast, when $t_s = 1000\,\text{ms}$, the robot performed poorly in both Canola Oil and Glycerin.

2) Undulation period experiment result: In order to evaluate the influence of the undulation period on the swimming performance, we fix the bistability-time $t_b = 0$ and let the robot swim in each environment for 30 s with 10 values of SMA activating time t_s. Figure 9 shows the swimming speed of our robot in Glycerin and Canola Oil. In the case of $t_s = 100\,\text{ms}$, for both swimming environments, as the SMA is extremely unstable, the robot could not undulate the entire running time (30 s). Therefore, we do not have the experimental result for that specific case.

It is evidently shown in Fig. 9 that in the case of swimming in a lower viscosity environment as Canola Oil, the robot excels at high frequency undulation. The robot reaches its maximum speed $V_{max} = 3.37\,\text{BL/min}$ at undulation period $T = 0.6\,\text{s}$ ($t_s = 300\,\text{ms}$). In contrast, when swimming in a higher viscosity environment as Glycerin solution, the robot reaches its top performance at low frequency undulation. The robot swimming in Glycerin achieve its maximum speed $V_{max} = 2.52\,\text{BL/min}$ at undulation period $T = 1.4\,\text{s}$ ($t_s = 700\,\text{ms}$). Fig. 10 shows the trajectories of the fastest and slowest robot in both swimming environment.

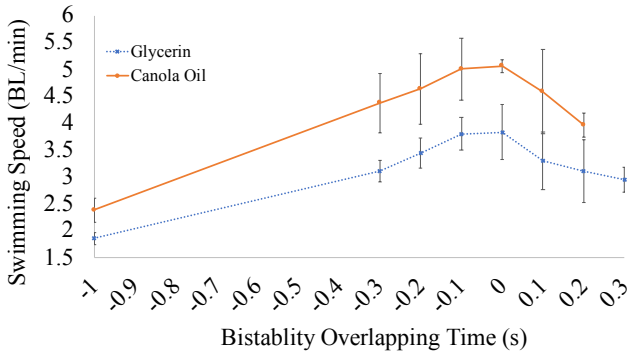

Fig. 11: The swimming speed ($\mathrm{BL/min}$) of our robot varies depending on the snap-through buckling of the deformable body.

3) Bistability on swimming speed experiment result: With the result from the previous experiment, we select the fastest robots for each swimming environment ($t_s = 700\,\mathrm{ms}$ for Glycerin and $t_s = 300\,\mathrm{ms}$ for Canola Oil) and change the bistability-time $t_b = bt_s$, with $b = \{-1.0, \pm 0.3, \pm 0.2, \pm 0.1, 0.0\}$. The swimming speeds of the robot in the two liquid environments are shown in Fig. 11. In both environments, the robots excel when the bistability-time is $t_b = 0$. This offset time between SMA (S_0, S_1) and (S_2, S_3) allow snap-through buckling to happen while still keeping the performance of the SMAs stable. When the bistability-time is set too high, which means there are too long overlapping between two opposite SMAs, the undulation of the body is unstable and thus jeopardizes the swimming speed of the robot. Especially when $t_b = 0.3t_s$, the Canola Oil swimmer becomes extremely unstable and barely swim at all. That is why we could not include the swimming speed of that case in Fig. 11. On the other hand, when the bistability-time is set too low, *e.g.* $t_b = -1.0t_s$, which means there is not any snap-through buckling happening along the body, the swimming speed of the robot is only about 50% that of the fastest cases. The trajectories of the robot with different bistability-time t_b in Fig. 12 and Fig. 13 confirm the stability of the swimming locomotion when $t_b = 0$.

B. Crawling

The experiment of crawling in this section is only aiming at confirming the possibility of terrestrial locomotion of our robot. There are plenty of rooms for improvement which are left for future works.

1) Experiment Setup: Our robot can crawl on a variety of surfaces as long as it can switch the touching points to the ground periodically. In this experiment, we use a flat paper surface to test the crawling locomotion gait. We also set the value of t_s and t_o in the same fashion as that in the swimming experiment. However, as the scope of the experiment, we only apply these parameters to the SMA pair (S_0 and S_2), which faces the crawling surface. While crawling, the SMAs are cooled off by surrounding air, which is slower than in

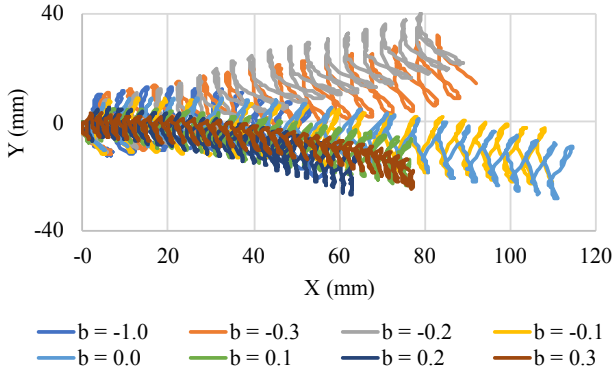

Fig. 12: Trajectories of the robot which swims in Glycerin solution with different bistability-time t_b.

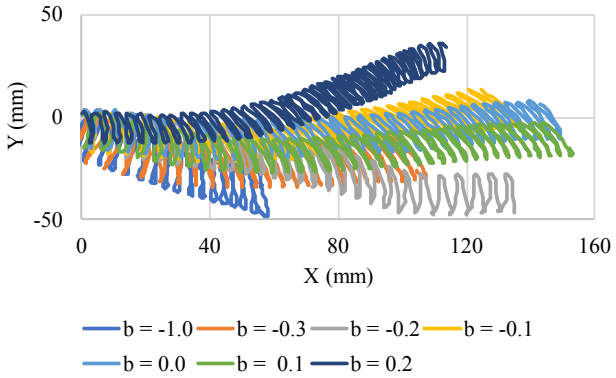

Fig. 13: Trajectories of the robot which swims in Canola Oil with different bistability-time t_b.

Canola Oil or Glycerin. Therefore, a prolonged activation time will burn the SMA quickly.

In the case of crawling, as we do not have to deal with the two-opposite-SMA situation, we can set $t_o = t_s$, *i.e.* the two SMA S_0 and S_2 are activated at the same time. As the SMAs take longer time to be cooled off in the air, we add an extra waiting time t_w to each crawling cycle. Through an empirical setup, we find out that with a $9\,\mathrm{V}$ power source, setting $t_s = 300\,\mathrm{ms}$, and $t_w = 3\,\mathrm{s}$ is good enough for the crawling of the robot on a flat paper surface.

2) Experiment Result: As shown in Fig. 14b, even without any optimization, our robot can crawl/inch on a flat paper surface. The trajectory is stably straight, and the crawling speed is $1.74\,\mathrm{BL/min}$. Fig. 14a shows that the alternations of the contact points between the robot and the ground are important for the crawling locomotion. In coordinating with the low friction head, the tail of the robot acts as a high frictional leg to push the body forward.

IV. DISCUSSION AND FUTURE WORKS

Due to the bi-stability soft-bodied structure, our robot can generate multigait locomotion. Especially, the swimming gait needs the snap-through buckling of the body to generate the undulation of the body, which is fast enough to propel the

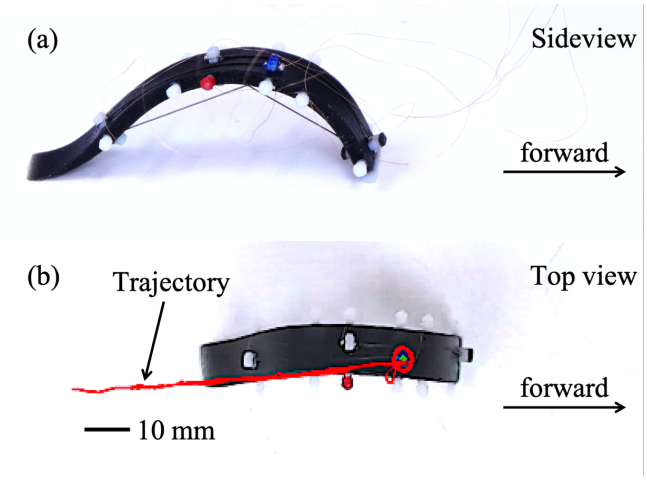

Fig. 14: (a) The robot is crawling on a paper surface. (b) The trajectory of the crawling robot in 20 s.

body forward. In the future, we can improve the performance of the robot as follows:

- *Customized body length and tail:* The robot is fixed length and tapered at its rear to form a thin tail. Optimization of the body length and the shape of the tail will support better swimming speed and give a deeper understanding of the influence of a tail on small swimmers.
- *Active buoyancy:* The robot uses passive Styrofoam spheres as buoyancy elements to help it float. It is possible to attach the robot with an active buoyancy system, which will enable the robot to control its depth in the liquid environment.
- *Circuit and SMA insulation:* Currently, the robot can only swim in insulator liquids, limiting its applications. Redesigning the body to house the SMAs and the circuit board insulatively will let the robot swim in a broader range of liquid environments.
- *Experiment in a wider variety of swimming environment*: To thoroughly understand the behavior of small swimmers, we will need more experiments of the robot swimming in a more comprehensive range of viscous settings.
- *Improvement of inching speed:* Our current robot moves on the terrestrial surface using only two SMAs. However, we have two extra SMAs on the dorsal side of the robot, which can work coordinately with the ventral side SMAs to increase the locomotion speed.
- *Theoretical model of the locomotion gaits:* It is generally challenging to model and simulate the fluid dynamic surrounding a small scale swimming robot. In this research, we focused on the experimental analysis of locomotion. By evaluating the performance of the robot in different viscous environments, we believe it laid a foundation for further theoretical analysis to understand the behavior of miniature swimmers in multiple viscous environments.

V. CONCLUSIONS

In this paper, we proposed a stringy robot that uses the soft-bodied bistability, incorporated with the active body segment overlapping, and frequency control to generate multi-gait locomotions. Our robot can crawl on the terrestrial area using inching gait and swim in a liquid environment using undulation of the slender body. The robot is miniaturized for better navigation in a spatially limited environment. We envision the robot not only for the environmental exploration but also as a model for studying the crawling and swimming of small creatures in different viscous environments.

ACKNOWLEDGMENT

This work was supported by JST ERATO Grant Number JPMJER1501, Japan, and Science of Softrobotics (18H05467), Japan, and JSPS and Grant-in-Aid for Scientific Research on Innovative Areas, The Ministry of Education, Culture, Sports, Science and Technology (MEXT), Japan.

REFERENCES

[1] G. Dudek, P. Giguere, C. Prahacs, S. Saunderson, J. Sattar, L. Torres-Mendez, M. Jenkin, A. German, A. Hogue, A. Ripsman, J. Zacher, E. Milios, H. Liu, P. Zhang, M. Buehler, and C. Georgiades, "AQUA: An amphibious autonomous robot," *Computer*, vol. 40, no. 1, pp. 46–53, Jan. 2007.

[2] Y. Chen, N. Doshi, B. Goldberg, H. Wang, and R. J. Wood, "Controllable water surface to underwater transition through electrowetting in a hybrid terrestrial-aquatic microrobot," *Nat. Commun.*, vol. 9, no. 1, p. 2495, Jun. 2018.

[3] B. B. Dey, S. Manjanna, and G. Dudek, "Ninja legs: Amphibious one degree of freedom robotic legs," in *2013 IEEE/RSJ International Conference on Intelligent Robots and Systems*, Nov. 2013, pp. 5622–5628.

[4] FESTO, "Bionicfinwave," Jul. 2018. [Online]. Available: https://www.festo.com/group/en/cms/13252.htm

[5] Pliant Energy Systems LCC, "Velox," Feb. 2018. [Online]. Available: https://www.pliantenergy.com/home-1

[6] A. Crespi, K. Karakasiliotis, A. Guignard, and A. J. Ijspeert, "Salamandra robotica II: An amphibious robot to study Salamander-Like swimming and walking gaits," *IEEE Trans. Rob.*, vol. 29, no. 2, pp. 308–320, Apr. 2013.

[7] A. Crespi and A. J. Ijspeert, "AmphiBot II: An amphibious snake robot that crawls and swims using a central pattern generator," in *Proceedings of the 9th international conference on climbing and walking robots (CLAWAR 2006)*, 2006, pp. 19–27.

[8] E. Kelasidi, K. Y. Pettersen, P. Liljebäck, and J. T. Gravdahl, "Locomotion efficiency of underwater snake robots with thrusters," in *2016 IEEE International Symposium on Safety, Security, and Rescue Robotics (SSRR)*, Oct. 2016, pp. 174–181.

[9] A. A. M. Faudzi, M. R. M. Razif, G. Endo, H. Nabae, and K. Suzumori, "Soft-amphibious robot using thin and soft McKibben actuator," in *2017 IEEE International Conference on Advanced Intelligent Mechatronics (AIM)*, Jul. 2017, pp. 981–986.

[10] Y. Tang, Q. Zhang, G. Lin, and J. Yin, "Switchable adhesion actuator for amphibious climbing soft robot," *Soft Robot*, vol. 5, no. 5, pp. 592–600, Oct. 2018.

[11] I. Borazjani and F. Sotiropoulos, "Numerical investigation of the hydrodynamics of carangiform swimming in the transitional and inertial flow regimes," *J. Exp. Biol.*, vol. 211, no. Pt 10, pp. 1541–1558, May 2008.

[12] M. C. Leftwich, E. D. Tytell, A. H. Cohen, and A. J. Smits, "Wake structures behind a swimming robotic lamprey with a passively flexible tail," *J. Exp. Biol.*, vol. 215, no. Pt 3, pp. 416–425, Feb. 2012.

[13] E. D. Tytell and G. V. Lauder, "The hydrodynamics of eel swimming: I. wake structure," *J. Exp. Biol.*, vol. 207, no. Pt 11, pp. 1825–1841, May 2004.

[14] Koichi Hirata, "Principles of the swimming fish robot," Feb. 2001. [Online]. Available: https://www.nmri.go.jp/oldpages/eng/khirata/fish/general/principle/index_e.html

[15] R. K. Katzschmann, J. DelPreto, R. MacCurdy, and D. Rus, "Exploration of underwater life with an acoustically controlled soft robotic fish," *Science Robotics*, vol. 3, no. 16, p. eaar3449, Mar. 2018.

[16] T. Li, G. Li, Y. Liang, T. Cheng, J. Dai, X. Yang, B. Liu, Z. Zeng, Z. Huang, Y. Luo, T. Xie, and W. Yang, "Fast-moving soft electronic fish," *Sci Adv*, vol. 3, no. 4, p. e1602045, Apr. 2017.

[17] C. Wilbur, W. Vorus, and Y. Cao, "A Lamprey-Based undulatory vehicle," *Neurotechnology for biomimetic robots*, pp. 285–296, 2002.

[18] A. Westphal, N. F. Rulkov, J. Ayers, D. Brady, and M. Hunt, "Controlling a lamprey-based robot with an electronic nervous system," pp. 39–52, 2011.

[19] A. D. Marchese, C. D. Onal, and D. Rus, "Autonomous soft robotic fish capable of escape maneuvers using fluidic elastomer actuators," *Soft Robot*, vol. 1, no. 1, pp. 75–87, Mar. 2014.

[20] G. Liu, Y. Ren, J. Zhu, H. Bart-Smith, and H. Dong, "Thrust producing mechanisms in ray-inspired underwater vehicle propulsion," *Theoretical and Applied Mechanics Letters*, vol. 5, no. 1, pp. 54–57, Jan. 2015.

[21] F. Berlinger, M. Duduta, H. Gloria, D. Clarke, R. Nagpal, and R. Wood, "A modular dielectric elastomer actuator to drive miniature autonomous underwater vehicles," in *2018 IEEE International Conference on Robotics and Automation (ICRA)*, May 2018, pp. 3429–3435.

[22] S. Mao, E. Dong, H. Jin, M. Xu, S. Zhang, J. Yang, and K. H. Low, "Gait study and pattern generation of a starfish-like soft robot with flexible rays actuated by SMAs," *J. Bionic Eng.*, vol. 11, no. 3, pp. 400–411, Sep. 2014.

[23] C. Rossi, J. Colorado, W. Coral, and A. Barrientos, "Bending continuous structures with SMAs: a novel robotic fish design," *Bioinspir. Biomim.*, vol. 6, no. 4, p. 045005, Dec. 2011.

[24] H. Shaw and A. Thakur, "Shape memory alloy based caudal fin for a robotic fish: Design, fabrication, control and characterization," in *Proceedings of the Advances in Robotics 2019*, ser. AIR 2019. New York, NY, USA: Association for Computing Machinery, 2019. [Online]. Available: https://doi.org/10.1145/3352593.3352666

[25] S.-H. Song, M.-S. Kim, H. Rodrigue, J.-Y. Lee, J.-E. Shim, M.-C. Kim, W.-S. Chu, and S.-H. Ahn, "Turtle mimetic soft robot with two swimming gaits," *Bioinspir. Biomim.*, vol. 11, no. 3, p. 036010, May 2016.

[26] R. F. Shepherd, F. Ilievski, W. Choi, S. A. Morin, A. A. Stokes, A. D. Mazzeo, X. Chen, M. Wang, and G. M. Whitesides, "Multigait soft robot," *Proc. Natl. Acad. Sci. U. S. A.*, vol. 108, no. 51, pp. 20 400–20 403, Dec. 2011.

[27] E. W. Hawkes, L. H. Blumenschein, J. D. Greer, and A. M. Okamura, "A soft robot that navigates its environment through growth," *Science Robotics*, vol. 2, no. 8, p. eaan3028, Jul. 2017.

[28] T. Umedachi and B. A. Trimmer, "Design of a 3d-printed soft robot with posture and steering control," in *2014 IEEE International Conference on Robotics and Automation (ICRA)*, May 2014, pp. 2874–2879.

[29] Hyunwoo Yuk, J. H. Shin, and Sungho Jo, "Design and control of thermal SMA based small crawling robot mimicking c. elegans," in *2010 IEEE/RSJ International Conference on Intelligent Robots and Systems*, Oct. 2010, pp. 407–412.

[30] J. Koh and K. Cho, "Omega-Shaped Inchworm-Inspired crawling robot with Large-Index-and-Pitch (LIP) SMA spring actuators," *IEEE/ASME Trans. Mechatron.*, vol. 18, no. 2, pp. 419–429, Apr. 2013.

[31] S. Nishikawa, Y. Arai, R. Niiyama, and Y. Kuniyoshi, "Coordinated use of Structure-Integrated bistable actuation modules for agile locomotion," *IEEE Robotics and Automation Letters*, vol. 3, no. 2, pp. 1018–1024, Apr. 2018.

[32] T. D. Ta, T. Umedachi, and Y. Kawahara, "Design of frictional 2D-Anisotropy surface for wriggle locomotion of printable soft-bodied robots," in *2018 IEEE International Conference on Robotics and Automation (IEEE ICRA'18)*. IEEE, May 2018, pp. 6779–6785.

[33] G. Ramel, "Fish muscles," Mar. 2020. [Online]. Available: https://www.earthlife.net/fish/muscles.html

[34] C. D. Onal and D. Rus, "Autonomous undulatory serpentine locomotion utilizing body dynamics of a fluidic soft robot," *Bioinspiration & Biomimetics*, vol. 8, no. 2, pp. 026 003–026 010, Jun. 2013.